EurJIC European Journal of Inorganic Chemistry

ChemPubSoc Europe

FULL PAPER

DOI:10.1002/ejic.201402711

Two Supramolecular Inorganic–Organic Hybrids of 12-Silicotungstic Acid Heteropolyoxometalate and Trinuclear Lanthanide Clusters: Syntheses, Structures, and Magnetic Properties

Nahid Lotfian,[a] Masoud Mirzaei,*[a] Hossein Eshtiagh-Hosseini,[a] Marta Löffler,[b] Maria Korabik,[b] and Alireza Salimi[a]

Keywords: Supramolecular chemistry / Polyoxometalates / Hydrothermal synthesis / Lanthanides / Magnetic properties

Hydrothermal synthesis of two novel inorganic–organic hybrid assemblies, $\{Na[Ln(pydc\text{-}OH)(H_2O)_4]_3\}[SiW_{12}O_{40}]\cdot 15H_2O$ [Ln = Nd (**1**) and Ln = Sm, (**2**); pydc-OH = 4-hydroxypyridine-2,6-dicarboxy], and their characterization is described. Structural characterizations by single-crystal X-ray diffraction reveal that these compounds are isostructural, and each consists of $[SiW_{12}O_{40}]^{4-}$ Keggin-type polyoxometalates (POMs) linked by three lanthanide ions to yield discrete trinuclear lanthanide clusters. These discrete molecules are further packed into 3D supramolecular assemblies by means of hydrogen-bonding and anion–π interactions. Both compounds exhibit remarkable thermal stability. The temperature variation in the magnetic susceptibility χ_m and of the $\chi_m T$ product and Bohr magnetons of the Nd^{III} (**1**)- and Sm^{III} (**2**)-based compounds are considered. The magnetic data have been interpreted relative to data presented in the literature.

Introduction

The targeted synthesis of inorganic–organic hybrid supramolecular materials through crystal engineering is a principal challenge of modern chemistry research.[1] These materials can exhibit specific macroscopic properties such as electronic, catalytic, sorbtive, separative, gas storage, and so forth, which originate from the synergistic interplay of the two microscopic components.[2] Furthermore, the properties and performance of hybrid compounds can potentially be improved and fine-tuned by incorporating suitable functionalities. One effective designed route to gain such functionalized hybrids is the extension of low-dimensional building blocks to high-dimensional networks between organic and/or inorganic molecular fragments on the basis of various forces including strong and directional interactions and weak intermolecular interactions. Polyoxometalates (POMs), as metal–oxygen cluster species, are significant inorganic components for this goal because of their extreme versatility of compositions, high structural stability, and infinite variety of chemical, physical, and biological properties.[3] Owing to their numerous surface oxygen atoms and various coordination modes, POMs have been viewed as inorganic multidentate ligands to coordinate with metal centers of the metal–organic skeleton, thus leading to the formation of compounds with diverse nuclearities that range from discrete oligonuclear to polymer species depending on the number of coordination sites and their geometric orientation.[4] For example, the relevance of POMs in molecular magnetism is based on the ability of these clusters to act as chelating ligands that incorporate a large number of magnetic centers at specific sites of their molecular structures.[5] Furthermore, plenty of oxygen atoms located on the surface of POMs offer better opportunities to form intermolecular weak interactions, including hydrogen bonds and anion–π interactions for constructing high-dimensional supramolecular architectures.[6] Among the continuously growing family of POM-based hybrids, POM-based lanthanide clusters are a very promising class of materials on account of their particular optical, Lewis acid catalytic, and magnetic properties.[7] However, the preparation of such structures is comparatively difficult since the oxophilic lanthanide cations possess high reactivity and can easily react with nucleophilic oxygen atoms on the surface of POMs, which usually results in fast precipitation instead of crystallization.[8] Moreover, the unavoidable competitive reactions between polyoxoanions and organic O-donor ligands with lanthanide ions lead to unpredictable results. Therefore, the organic ligands, owing to their different steric effects, structure, and degree of softness/rigidity, can control and adjust the structural assembly. It was found that the introduction of aro-

[a] Department of Chemistry, Ferdowsi University of Mashhad, 917751436 Mashhad, Iran
E-mail: mirzaeesh@um.ac.ir
mirzaeesh.profcms.um.ac.ir
[b] Faculty of Chemistry, University of Wrocław, F. Joliot-Curie 14, 50-383 Wrocław, Poland

Supporting information for this article is available on the WWW under http://dx.doi.org/10.1002/ejic.201402711.

© 2014 Wiley-VCH Verlag GmbH & Co. KGaA, Weinheim

matic multicarboxylic ligands into the Ln–POM system is valuable on account of the rigidity of the aromatic part, which favors the formation of ordered single crystals, and the high affinity of carboxylate function and lanthanide ions.[9] As a striking example, pyridine-2,6-dicarboxylic acid (H_2pydc) has received more extensive attention in the construction of POM-based lanthanide clusters.[10] The small size of this ligand might help to reduce steric hindrance and encourage further connectivity, which can usually cause an increase in the extra-framework volume of new porous 3D network fittings for wrapping POM clusters. Recently, a series of compounds constructed from pyridine-2,6-dicarboxylic acid−Keggin POMs $[XM_{12}O_{40}]^{n-}$ (M = Mo, W; X = Si, Ge, P) with Ln = La, Ce, Pr, Nd, Sm, Eu, Gd, Tb, Dy, Tm; and also $[PMo_{12-x}V_xO_{40}]^{(3+x)-}$ (x = 1, 2) with Ln = La, Ce, Pr, Nd, Sm−have been reported by several research groups.[11] All these compounds consist of a zeolite-like four-connected three-dimensional cationic framework $\{[Ln(H_2O)_4(pydc)]_4\}^{4+}$ and ball-shaped Keggin-type templates. These investigations led us to wonder how the structures might be tuned while using the derivatives of H_2pydc with almost an similar coordination mode but different steric hindrance and electron delocalization. Therefore, to explore the effect of hydroxy group at the 4-position of the H_2pydc ligand on the resultant products, we chose to assemble 4-hydroxypyridine-2,6-dicarboxylic acid (H_2pydc-OH) with lanthanide ions and $[SiW_{12}O_{40}]^{4-}$ Keggin-type POMs. Similar conditions can result in completely different structures with novel prospects (Scheme 1).

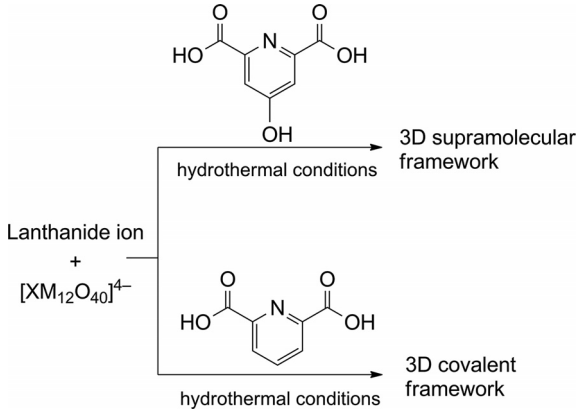

Scheme 1. Structural differences in products of OH-pydc and pydc ligands.

In this work, we present the hydrothermal synthesis and characterization of two novel lanthanide inorganic–organic hybrids, namely, $\{Na[Ln(pydc\text{-}OH)(H_2O)_4]_3\}[SiW_{12}O_{40}]\cdot 15H_2O$ [Ln = Nd, (**1**) and Ln = Sm, (**2**); pydc-OH = 4-hydroxypyridine-2,6-dicarboxy]. These compounds are isostructural, and each one displays a trinuclear Ln–organic cluster, which is bound to three terminal oxygen atoms of the $[SiW_{12}O_{40}]^{4-}$ moiety. These two compounds are discrete molecules and are further connected by hydrogen bonds and anion–π interactions to construct a 3D supramolecular network. As far as we know, these compounds represent the first examples of POM-supported symmetric trinuclear Nd and Sm clusters. In addition, investigation of the influence of the anion–π interaction on the solid-state structure of the POM-based hybrid inorganic–organic frameworks is unprecedented. Furthermore, the coordination mode of the Keggin used in these structures has previously been very rarely reported.

Results and Discussion

Synthesis

Compounds **1** and **2** were synthesized under similar hydrothermal conditions. The conditions reported in the Exp. Sect. were optimized for yields of pure crystalline products. In our experiments, the pH values were kept at 3.5–4 for both compounds, and beyond that pH range no products were obtained or the yield was low. It has been shown that the presence of the Na ion in heterometallic clusters affects the formation of final structures by adjusting the pH of the base. For these reaction systems, the reaction temperature was optimized to be within the range of 110–120 °C. As the synthesis temperature increased above 120 °C, the quality of the crystals decreased, which might be due to the loss of water molecules at higher temperatures.[12]

It is noteworthy that our attempts to obtain similar structures by replacing 4-hydroxypyridine-2,6-dicarboxylic acid (pydc-OH) with pyridine-2,6-dicarboxylic acid (pydc) led to the formation of the reported 3D covalent framework instead of the 3D supramolecular framework (Scheme 1).[11] These results indicate that the hydroxy group might produce steric hindrance and force the compound to have a lower dimension, therefore compounds **1** and **2** with discrete supramolecular structures were achieved.

IR Spectroscopy

The characteristic vibration patterns in the IR spectra of **1** and **2** are similar (Figures S1a and S1b in the Supporting Information). This suggests that they are isostructural, and X-ray structural analyses results confirm this assumption. In the low-wavenumber region (<1000 cm^{-1}), compounds **1** and **2** exhibit four identical characteristic bands at 924, 975, 882, and 797 cm^{-1}, attributed to ν_{as}(Si–O), ν_{as}(W–O_t), ν_{as}(W–O_b), and ν_{as}(W–O_c) of the α-Keggin $[SiW_{12}O_{40}]^{4-}$ POMs (for which O_t = terminal oxygen, O_b = bridged oxygen of two octahedral sharing a corner, O_c = bridged oxygen of two octahedral sharing edges), respectively. Relative to the typical Keggin-type parent $[\alpha\text{-}SiW_{12}O_{40}]^{4-}$,[13] the vibration bands are almost unshifted, which suggests that the coordination of the $\{Na[Ln(pydc\text{-}OH)(H_2O)_4]\}^{4+}$ cation to terminal oxygen atoms of the Keggin anion has a weak influence on the terminal oxygen atoms of $[SiW_{12}O_{40}]^{4-}$ fragments. In the middle of the stretching vibrations (1000–1750 cm^{-1}), the IR results have been employed to distinguish the coordination modes of organic ligand. The bands of 1254 and 1246 cm^{-1} in **1** and **2**, respectively, correspond

 © 2014 Wiley-VCH Verlag GmbH & Co. KGaA, Weinheim

to the ν(ArC–OH), which indicates that the hydroxy oxygen atoms do not coordinate with the lanthanide ions. The ν_s(C=N) stretching vibration of the pyridine ring with medium intensity appears at 1340 cm^{-1} for **1** and 1342 cm^{-1} for **2**. The absence of ν(C=O) bands at 1727 cm^{-1} in both spectra confirms that all carboxyl groups of H_2pydc-OH ligands are deprotonated and coordinated to the lanthanide ions. The vibrations of the carboxylate groups are at 1429 (**1**) and 1431 cm^{-1} (**2**) for the symmetric stretching and at 1573, 1601 (**1**) and 1573, 1603 cm^{-1} (**2**) for the asymmetric stretching. The splitting of ν_{as}(COO) into two bands suggests that the two carboxylate groups are in different coordination environments. Finally, a broad feature around 3450 cm^{-1} is assigned to the ν(OH) vibration of coordinated and crystalline water molecules. The broadness of this band is representative of strong hydrogen-bonding interactions in the crystal structure. In summary, these results are in good agreement with X-ray crystallography results and offer further proof of the structures.

Structural Description

X-ray structural analyses established that compounds **1** and **2** possess a crystallographic C_3 axis and crystallize in the chiral space group *R*3 (trigonal system) with Flack parameters of 0.03(3) and 0.00(3), respectively. Thus, only a third of the molecule is located in the asymmetric unit. These compounds are isostructural and only minor differences exist owing to the different radii of Nd and Sm, so that the following description focuses on the crystal structure of **2**. The basic structural unit of compound **2** is composed of a heterometallic cluster $\{Na[Sm(pydc\text{-}OH)(H_2O)_4]_3\}^{4+}$, a $[SiW_{12}O_{40}]^{4-}$ polyoxoanion, and fifteen crystalline water molecules (Figure 1, a). The polyoxoanion $[SiW_{12}O_{40}]^{4-}$ exhibits the typical Keggin configuration, in which the central SiO_4 tetrahedron is surrounded by four vertex-sharing W_3O_{13} trimers. All tungsten atoms have a $\{WO_6\}$ octahedral environment, and according to the kind of oxygen atom bonded to the tungsten atoms, the W–O bond lengths are divided into three groups. The W–O_c bond lengths (O_c = center oxygen atom) are the longest [2.33(2)–2.37(2) Å], the W–O_b bond lengths (O_b = bridge oxygen atom) are intermediate [1.84(2)–1.97(2) Å], and the W–O_t bond lengths (O_t = terminal oxygen atom) are the shortest [1.69(2)–1.75(2) Å]. The Si–O bond lengths are in the range 1.59(4)–1.65(2) Å. All W–O and the central Si–O distances correspond to those in the literature.[14] As shown in Figure 2 (a), the $[SiW_{12}O_{40}]^{4-}$ anion can be viewed as a tridentate inorganic ligand that bonds to three samarium ions through terminal O atoms to generate a trinuclear samarium cluster. An interesting structural feature of **2** is that all coordinating O atoms belong to a corner-sharing W_3O_{15} triad, thereby resulting in a discrete molecule. To the best of our knowledge, this uncommon coordination pattern of a Keggin-type polyoxoanion is still relatively scarce.[4a] A view of the samarium cluster is represented in Figure 1 (b). In **2**, the presence of a C_3 axis requires the Sm centers to be crystallographically equivalent. The Sm^{III} ions define the corners of an equilateral triangle and are connected through a carboxylate oxygen from 4-hydroxypyridine-2,6-dicarboxy, with a side of about 6.653 Å. Each Sm ion is nine-coordinated and exhibits monocapped square-antiprism geometry (Figure 2, b), namely, three carboxylate oxygen atoms from two pydc-OH^{2-} ligands [Sm–$O_{carboxylate}$ 2.36(3)–2.47(2) Å], one nitrogen atom of the pyridine rings [Sm–N 2.49(3) Å], one terminal oxygen atom from the W12 subunit [Sm–O_{POM} 2.49(2) Å], and four water molecules [Sm–O_{water} 2.45(3)–2.59(2) Å]. As shown in Table 1, the variation in Sm–O bond lengths consists of the following sequence: Sm–O_{water} > Sm–O_{POM} > Sm–O_{ligand}, which in-

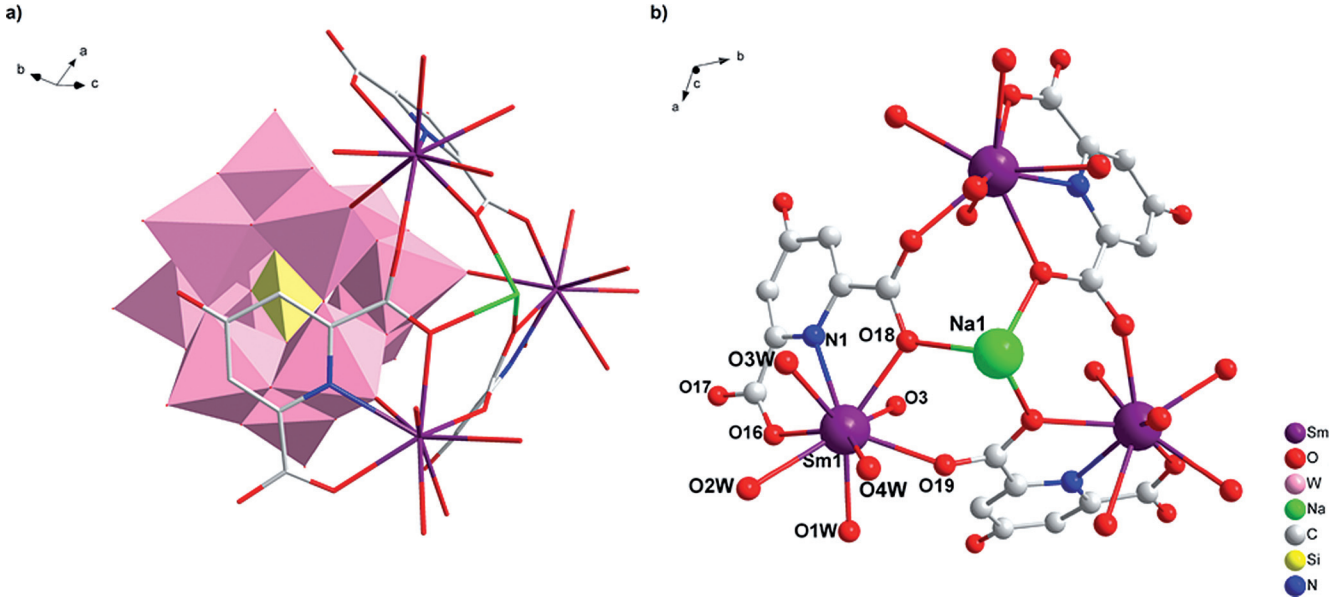

Figure 1. (a) View of the molecular structure of **2**. (b) Structure of the trinuclear samarium cluster. Crystalline water molecules and hydrogen atoms are omitted for clarity.

 © 2014 Wiley-VCH Verlag GmbH & Co. KGaA, Weinheim

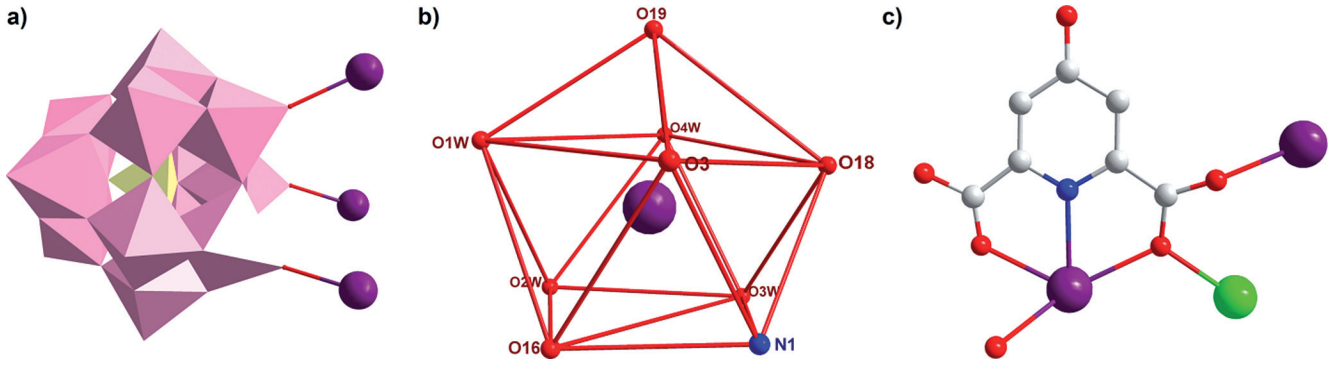

Figure 2. (a) Coordination sites of Keggin POM. (b) Monocapped square antiprism geometry of Sm^{3+}. (c) Coordination number and modes of the OH-pydc ligand.

dicates that the electron-donating ability of oxygen atoms is in the order of $O_{ligand} > O_{POM} > O_{water}$, and that the Sm–$O_{ligand}$ bonds are more stable than the Sm–O_{water} or Sm–O_{POM} bonds. In the coordination configuration of Sm^{3+}, the O3, O18, O1W, and O4W group and the O16, N1, O2W, and O3W group define the two square faces of the square antiprism with an angle of 3.25° for the two planes. The distances of the Sm1 center and the two bottom planes are 0.802 and 1.531 Å, respectively. O19 occupies the cap position, and the distances between O19 and the two bottom planes are 1.549 and 3.887 Å, respectively. These data indicate that the square-antiprismatic geometry of Sm^{3+} is distorted. Interestingly, the sodium ions are found trapped in the center of the trinuclear Sm cluster, which is located on the C_3-symmetry axis and lies below the Sm_3 plane of 1.485 Å. Although heterometallic structures based on 3d–4f assemblies are often encountered, such a network based on 4f metal and main-group elements is really infrequent.[15] Furthermore, as can be seen in Figure 1 (b), this central

Table 1. Selected bond lengths [Å] for **1** and **2**.[a]

	Ln = Nd^{+} (**1**)	Ln = Sm^{3+} (**2**)
Ln–O3	2.55(2)	2.49(2)
Ln–O16	2.43(2)	2.43(2)
Ln–O18	2.47(3)	2.47(2)
Ln–O19^{i}	2.36(3)	2.36(3)
Ln–N1	2.53(3)	2.49(3)
Ln–O1W	2.58(3)	2.45(3)
Ln–O2W	2.53(3)	2.54(3)
Ln–O3W	2.52(3)	2.59(2)
Ln–O4W	2.51(3)	2.50(2)
Avg. Ln–O(ligand)	2.45	2.44
Avg. Ln–O(H_2O)	2.54	2.52
Avg. Ln–O	2.49	2.48

[a] Symmetry code: (i) $1 - y, 1 + x, z$.

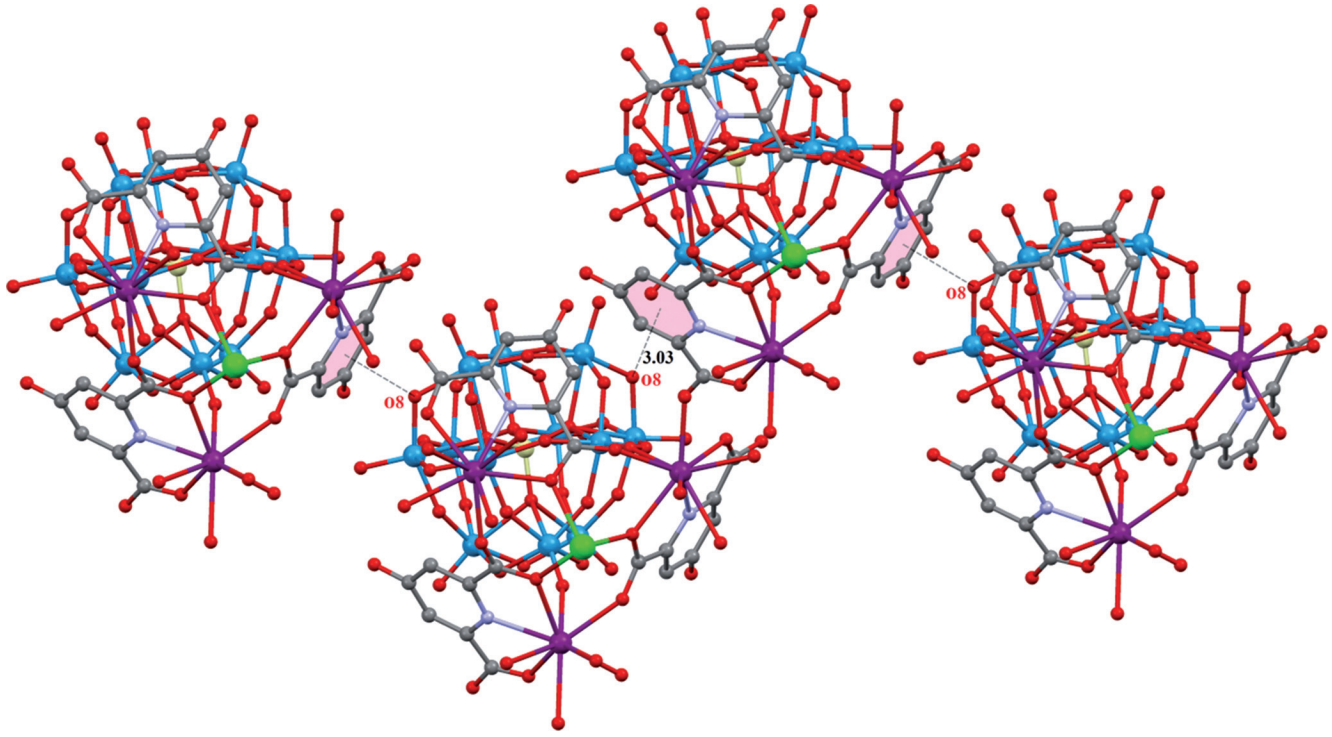

Figure 3. Partial view of the crystal packing of compound **2** with indication of the intermolecular anion–π interaction established between the organic ligand and O8 of the Keggin.

 © 2014 Wiley-VCH Verlag GmbH & Co. KGaA, Weinheim

sodium ion is rarely three-coordinated by three μ_3-O atoms of carboxylate groups of three ligands. It should be noted that each pydc-OH in **2** acts as both a chelating and bridging ligand and binds three cations (two equivalent Sm^{3+} and one Na^+) in a pentadentate fashion. The unique asymmetric coordination mode of the ligand is shown in Figure 2 (c), in which one carboxylate group adopts a monodentate coordination fashion to coordinate one Sm^{3+} ion, whereas the other carboxylate group behaves like a μ_3-linker with the O18 oxygen atom, which bridges Sm^{3+} and Na^+, whereas the O19 oxygen atom connects to another Sm^{3+} ion. The phenolic hydroxy oxygen atom does not participate in the coordination owing to protonation.

In the packing arrangement, the anion–π interactions and hydrogen bonds connect the discrete molecules into a 3D supramolecular framework. As shown in Figure 3, the O8 bridging oxygen atoms of the Keggin moieties are oriented toward the π face of pyridine rings of neighboring units. The distances between O8 atoms and the centroid of the pyridine rings are 3.034 Å, which is considerably shorter than the sum of van der Waals radii (3.22 Å) and thus a clear indication of binding.[16] This interaction can be also viewed as a lone pair (lp)–π interaction in which one free lone pair of O8 bridging atom is pointing toward the π face of the pyridine that it is coordinated to the metal that enhances its π acidity. Figure 4 shows how the terminal oxygen atoms (O5, O9, O11, and its symmetry equivalents) of Keggin and hydroxy groups of organic ligands from one molecular unit interact with the oxygen atoms of coordinated water (O1W, O2W, O3W, and its symmetry equivalents) from the neighboring units through hydrogen bonds to form a 3D flowerlike supramolecular network. The representing short distances [Å] are O5···O1W 2.82(4), O9···O2W 2.70(4), O9···O3W 3.01(4), O11···O2W 2.97(4), and O17···O4W 2.89(4). The crystalline water molecules reside as guests in the interspaces of the 3D supramolecular framework through extensive hydrogen-bonding interactions. All of these contacts make the crystal structure more stable. The Ln–O and Ln–N bond lengths in the crystals of **1** and **2** have been shown in Table 1.

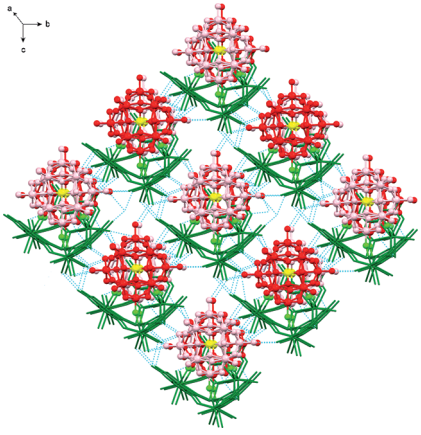

Figure 4. A view of the 3D supramolecular structure in **2**.

Thermal Analysis

The thermal stability of compounds **1** and **2** was studied by means of thermogravimetric analysis (TGA) and differential scanning calorimetry (DSC) under an air atmosphere from 20 to 950 °C. The TG/DSC curves for **1** and **2** are provided in Figures S2 and S3 of the Supporting Information. Compounds **1** and **2** both exhibit similar weight-loss stages. TGA of compound **2** shows 11.18% weight loss between 20 and 328 °C, which is attributed to the loss of 15 crystalline and 12 coordinated water molecules, and remains in good agreement with the calculated value of 11.12%. In the corresponding DSC curve, there is an endothermic peak at 111 °C. The 4.28% weight loss (calculated value: 4.65%) from 328 to 530 °C is considered to be the release of one OH-pydc molecule. Then, the 9.42% weight loss (calculated value: 9.76%) in the temperature range of 530–690 °C has been ascribed to the decomposition of two other OH-pydc ligands. Correspondingly, three exothermic peaks are observed at 455, 585, and 637 °C in the DSC curve, respectively, which arise from the combustion of OH-pydc ligands. The total weight loss of 22.84% (calculated: 22.30%) indicates that the final products have $Sm_3NaSiW_{12}O_{43}$ composition, and this could be $3/2Sm_2O_3 + 1/2Na_2O + SiO_2 + 12WO_3$ or $(SmNa)WO_4 + Sm_2(WO_4)_3 + SiO_2 + 8WO_3$ as well.

Magnetic Properties

Magnetization measurements in the temperature range of 1.8–300 K were carried out on powdered crystals of compounds, at a magnetic field of 0.5 T. Corrections for diamagnetism of the constituting atoms were calculated using Pascal's constant.[17] The effective magnetic moments were calculated from the following expression: $\mu_{eff} = 2.83\sqrt{\chi_m^{corr} \cdot T}$ (B.M.).

The temperature variation of the magnetic susceptibility χ_m and of the $\chi_m T$ product of the Nd^{III} (**1**)- and Sm^{III} (**2**)-based compounds is displayed in Figure 5. The magnetic data have been interpreted in comparison to data presented in the literature.[17b,18] On cooling, $\chi_m T$ values of **1** gradually decrease, and the χ_m^{-1} versus T data for **1** obeys the Curie–Weiss law in the range 100–300 K (**1** in Figure 5, inset), with $C = 1.94\ cm^3\,K\,mol^{-1}$. Such behavior is typical of isolated Nd^{III} coordination compounds, in which only the ground state of free Nd^{III} ions ($^4I_{9/2}$) is populated, even at room temperature. The first excited state is located at above approximately 2000 cm^{-1} (at 1400 K).[7e,17b,18a] For Nd^{III} ions, spin–orbital coupling, λ, is very large—$S = 3/2$, $L = 6$, $g = 8/11$[17b,18a]—which leads to $\chi_m T = 1.64\ cm^3\,K\,mol^{-1}$. The experimental room temperature value of $1.60\ cm^3\,K\,mol^{-1}$ ($\mu_{eff} = 3.58$ B.M.) agrees with this value. Below 100 K, a steeper decrease of $\chi_m T$ is observed as a combined effect of thermal population of the Stark levels[17b,18a–18e] modulated by the crystal field and the molecular symmetry of the compound.

© 2014 Wiley-VCH Verlag GmbH & Co. KGaA, Weinheim

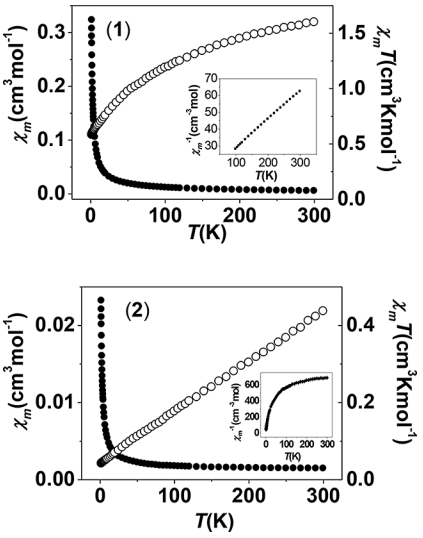

Figure 5. Variable-temperature magnetic susceptibilities of complexes (**1**) and (**2**) in the form of χ_m (●) and $\chi_m T$ (○) versus T (χ_m calculated per one Ln^{III} center). The insets show the temperature dependence of reciprocal magnetic susceptibility.

The magnetism of compound **2** is more complex. In the case of Sm^{III} ions the spin–orbital coupling parameter, λ, is on the order of 200 cm^{-1},[17b] the ground ^{6}H term is split into six levels, from $^6H_{5/2}$ (S = 5/2, L = 5, g = 2/7) to $^6H_{15/2}$, and several excited states might be populated at room temperature.[17b,18a,18d–18j] As a consequence, the presence of low-lying excited states adds a significant temperature-independent contribution to the magnetic susceptibility, and the experimental $\chi_m T$ (scaled per one Sm^{III} center), which was determined to be about 0.457 cm^3 K mol^{-1} (μ_{eff} = 1.91 B.M.), at 300 K is higher than expected in the free-ion approximation of 0.09 cm^3 K mol^{-1}.[17b,18f–18j] Decreasing the temperature leads to a depopulation of excited states, and a systematically linear decrease in $\chi_m T$ with the lowering of temperature to 0.042 cm^3 K mol^{-1} (μ_{eff} = 0.58 B.M.) at 1.8 K was observed in the experimental data. The χ_m^{-1} versus T data for compound **2** do not obey the Curie–Weiss law over the whole measured region (**2** in Figure 5, inset).

Conclusion

In the present work, we succeeded in synthesizing two novel inorganic–organic hybrid compounds based on lanthanide clusters and Keggin POMs by means of a hydrothermal method. The results demonstrate that the unique coordination modes of the Keggin anions and the pydc-OH ligands play important roles in the formation of the discrete trinuclear lanthanide structure with a central sodium ion. Interestingly, these discrete molecules are linked together through hydrogen-bonding and anion–π interactions, which forms the 3D supramolecular framework. The magnetic properties are in agreement with isolated Nd^{III} and Sm^{III} ions in the solid state, and they show the usual temperature-dependent behavior with the gradual depopulation of the Stark levels. Investigations of the gas storage, separation, and catalytic properties of these novel synthesized species are in progress, and the results will be reported in due time.

Experimental Section

General Methods and Materials: All reagents were commercially purchased and used without further purification. The FTIR spectra were recorded in the range 4000–400 cm^{-1} with an Avatar 370 Thermo Nicolet spectrometer using KBr pellets. The C, H, and N elemental analyses were performed with a Thermo Finnigan Flash model 1112EA microanalyzer. Thermogravimetric analyses and differential scanning calorimetry were carried out under an air atmosphere between 30 and 950 °C at a heating rate of 10 °C min^{-1} with a TG-DTA Setaram SETSYS 16/18. Magnetization measurements in the temperature range of 1.8–300 K were carried out for samples of powdered crystals of complexes **1** and **2** (**1** 51.08, **2** 26.1 mg) at a magnetic field of 0.5 T with a Quantum Design SQUID Magnetometer (type MPMS-XL5). The magnetic data were corrected for the sample holder (Quantum Design Clear Plastic Straws in Paper - AGC2, free of paramagnetic impurities).

Synthesis of 1: A mixture of $H_4SiW_{12}O_{40}{\cdot}nH_2O$ (288 mg, 0.1 mmol), $Nd(NO_3)_3{\cdot}6H_2O$ (110 mg, 0.25 mmol), H_2pydc-OH·H_2O (50 mg, 0.25 mmol), and H_2O (15 mL) was stirred for about an hour or so. When the pH of the mixture was adjusted to about 4 with an NaOH solution, the mixture was transferred into a Teflon-lined autoclave and kept under autogenous pressure at 120 °C for 3 d. After slow cooling to room temperature, yellow prismatic crystals of **1** were obtained in a 55% yield based on $H_4SiW_{12}O_{40}$. $C_{21}H_{63}N_3NaNd_3O_{82}SiW_{12}$ (4359.70): calcd. C 5.79, H 1.46, N 0.96, Si 0.64, W 50.60, Nd 9.92; found C 5.85, H 1.42, N 0.89, Si 0.64, W 50.44, Nd 9.85. IR (KBr pellet): $\tilde{\nu}$ = 3419 (br. s), 1601 (s), 1573 (s), 1491 (w), 1429 (s), 1340 (m), 1246 (m), 1123 (m), 1029 (s), 975 (s), 924 (s), 882 (m), 797 (s), 702 (w), 634 (w), 688 (w), 533 (m) cm^{-1}.

Synthesis of 2: Compound **2** was prepared similarly to **1**, except that $Sm(NO_3)_3{\cdot}6H_2O$ (111 mg, 0.25 mmol) was used in place of $Nd(NO_3)_3{\cdot}6H_2O$. Yellow prismatic crystals were obtained in a 63% yield based on $H_4SiW_{12}O_{40}$. $C_{21}H_{63}N_3NaO_{82}SiSm_3W_{12}$ (4378.18): calcd. C 5.76, H 1.45, N 0.96, Si 0.66, W 50.38, Sm 10.30; found C 5.75, H 1.43, N 0.90, Si 0.63, W 50.27, Sm 10.22. IR (KBr pellet): $\tilde{\nu}$ = 3471 (br. s), 1603 (s), 1573 (s), 1491 (w), 1431 (s), 1342 (s), 1254 (w), 1119 (w), 1031 (s), 975 (s), 924 (s), 882 (m), 797 (s), 702 (w), 637 (w), 584 (w), 530 (m) cm^{-1}.

X-ray Crystallography: X-ray data for compounds **1** and **2** were collected with a STOE-IPDS-II diffractometer with graphite-monochromated Mo-K_α radiation (λ = 0.71073 Å). Suitable crystals were chosen with a polarizing microscope for X-ray single-crystal diffraction experiments, covered with oil, and were mounted on a glass fiber that was used for data collection. Crystallographic data were collected at a temperature of 120(2) K to a maximum 2θ value of 56.78° for **1** and at a temperature of 298(2) K to a maximum 2θ value of 51.50° for **2**, and in an a series of ω scans in 1° oscillations and integrated by using the Stoe X-AREA software package.[19] Numerical absorption corrections were performed using the analytical procedure included in the WinGX program suite.[20] The structures were solved by direct methods[21] and subsequent difference Fourier maps and then refined on F^2 by a full-matrix least-squares procedure using anisotropic displacement parameters. The structures were checked for higher symmetry with the help of the PLATON program.[22] For all compounds, the non-

 © 2014 Wiley-VCH Verlag GmbH & Co. KGaA, Weinheim

hydrogen atoms were refined anisotropically and hydrogen atoms were placed in ideal positions. Oxygen atoms O5W, O7W, and O8W of water molecules in the case of compound **2** were refined isotropically. Hydrogen atoms from water molecules could not be located in difference Fourier maps. The structural resolution procedure was conducted using the WinGX crystallographic software package. A summary of crystallographic data and structural refinement can be seen in Table 2.

Table 2. Crystallographic data and structure refinement for **1** and **2**.

	1	**2**
Empirical formula	$C_{21}H_{63}Nd_3N_3NaO_{82}SiW_{12}$	$C_{21}H_{63}Sm_3N_3NaO_{82}SiW_{12}$
M_r	4359.62	4377.98
T [K]	120(2)	298(2)
Crystal size [mm^3]	0.25×0.15×0.15	0.30×0.20×0.15
Crystal system	trigonal	trigonal
Space group	*R*3	*R*3
a, b [Å]	18.0861(8)	18.0770(9)
c [Å]	20.9915(10)	20.9341(10)
α, β [°]	90	90
γ [°]	120	120
V [Å^3]	5946.5(5)	5924.3(5)
Z	3	3
$D_{calcd.}$ [g cm^{-3}]	3.607	3.636
θ range [°]	2.25–28.39	2.34–25.75
μ [mm^{-1}]	19.408	19.729
F(000)	5715.0	5733.0
Reflections collected	4756	3641
Final R_1[a], wR_2[b] [$I>2\sigma(I)$]	0.0758, 0.1966	0.0583, 0.1524
GoF	1.057	1.088

[a] $R_1 = \Sigma||F_o| - |F_c||/\Sigma|F_o|$. [b] $wR_2 = \{\Sigma w(F_o^2 - F_c^2)^2/\Sigma w(F_o^2)^2\}^{1/2}$.

CCDC-995731 (for **1**) and -995732 (for **2**) contain the supplementary crystallographic data for this paper. These data can be obtained free of charge from The Cambridge Crystallographic Data Centre via www.ccdc.cam.ac.uk/data_request/cif.

Supporting Information (see footnote on the first page of this article): IR spectra and TGA/DSC curves.

Acknowledgments

This work was financially supported by the Ferdowsi University of Mashhad (grant number 18768/3-2011/10/04) and by the Polish National Science Centre (grant number NN204 198240).

[1] a) *Hybrid Materials: Synthesis Characterization, and Applications* (Ed.: G. Kickelbick), Wiley-VCH, Weinheim, Germany, **2007**; b) L. Carlucci, G. Ciani, D. M. Proserpio, *Coord. Chem. Rev.* **2003**, *246*, 247; c) P. J. Steel, *Acc. Chem. Res.* **2005**, *38*, 243; d) C. Streb, T. McGlone, O. Brücher, D. L. Long, L. Cronin, *Chem. Eur. J.* **2008**, *14*, 8861; e) S. Kennedy, G. Karotsis, C. M. Beavers, S. J. Teat, E. K. Brechin, S. J. Dalgarno, *Angew. Chem. Int. Ed.* **2010**, *49*, 1; *Angew. Chem.* **2010**, *122*, 1; f) T. R. Amarante, P. Neves, A. C. Gomes, M. M. Nolasco, P. R. Claro, A. C. Coelho, A. A. Valente, F. A. Almeida Paz, S. Smeets, L. B. McCusker, M. Pillinger, I. S. Gonçalves, *Inorg. Chem.* **2014**, *53*, 2652.

[2] a) C. P. Collier, E. W. Wong, M. Belohradský, F. M. Raymo, J. F. Stoddart, P. J. Kuekes, R. S. Williams, J. R. Heath, *Science* **1999**, *285*, 391; b) C. D. Wu, A. Hu, L. Zhang, W. Lin, *J. Am. Chem. Soc.* **2005**, *127*, 8940; c) A. Lesbani, R. Kawamoto, S. Uchida, N. Mizuno, *Inorg. Chem.* **2008**, *47*, 3349; d) K. Shin, Y. Kim, T. A. Strobel, P. S. R. Prasad, T. Sugahara, H. Lee, E. D. Sloan, A. K. Sum, C. A. Koh, *J. Phys. Chem. A* **2009**, *113*, 6415; e) C. Sanchez, P. Belleville, M. Popalld, L. Nicoleab, *Chem. Soc. Rev.* **2011**, *40*, 696; f) M. L. Foo, R. Matsuda, S. Kitagawa, *Chem. Mater.* **2014**, *26*, 310.

[3] a) M. T. Pope, *Heteropoly and Isopoly Oxometalates*, Springer, Berlin, **1983**; b) D. L. Long, E. Burkholder, L. Cronin, *Chem. Soc. Rev.* **2007**, *36*, 105; c) C. Ritchie, A. Ferguson, H. Nojiri, H. Miras, Y. F. Song, D. L. Long, L. Cronin, *Angew. Chem. Int. Ed.* **2008**, *47*, 5609; *Angew. Chem.* **2008**, *120*, 5691; d) R. Tsunashima, D. L. Long, H. N. Mira, D. Gabb, C. P. Pradeep, L. Cronin, *Angew. Chem. Int. Ed.* **2010**, *49*, 113; *Angew. Chem.* **2010**, *122*, 117; e) J. Zhang, J. Hao, Y. G. Wei, F. P. Xiao, P. C. Yin, L. S. Wang, *J. Am. Chem. Soc.* **2010**, *132*, 14; f) Y. Hu, F. Luo, F. F. Dong, *Chem. Commun.* **2011**, *47*, 761; g) K. Uehara, N. Mizuno, *J. Am. Chem. Soc.* **2011**, *133*, 1622; h) H. Stephan, M. Kubeil, F. Emmerling, C. E. Müller, *Eur. J. Inorg. Chem.* **2013**, 1584.

[4] a) J. Sha, J. Peng, H. Liu, J. Chen, B. Dong, A. Tian, Z. Su, *Eur. J. Inorg. Chem.* **2007**, 1268; b) J. W. Zhao, B. Li, S. T. Zheng, G. Y. Yang, *Cryst. Growth Des.* **2007**, *7*, 2658; c) L. Dai, W. You, E. Wang, S. Wu, Z. Su, Q. Du, Y. Zhao, Y. Fang, *Cryst. Growth Des.* **2009**, *9*, 2110; d) H. Yang, S. Gao, J. Lu, B. Xu, J. Lin, R. Cao, *Inorg. Chem.* **2010**, *49*, 736; e) X. Y. Wu, Q. K. Zhang, X. F. Kuang, W. Y, R. M. Yu, C. Z. Lu, *Dalton Trans.* **2012**, *41*, 11783; f) X. L. Wang, Q. Gao, A. X. Tian, G. C. Liu, *Cryst. Growth Des.* **2012**, *12*, 2346; g) G. Rousseau, E. Rivière, A. Dolbecq, J. Marrot, O. Oms, P. Mialane, *Eur. J. Inorg. Chem.* **2013**, 1793; h) M. Mirzaei, H. Eshtiagh-Hosseini, M. Alipour, A. Frontera, *Coord. Chem. Rev.* **2014**, *275*, 1.

[5] a) U. Kortz, A. Müller, J. Van Slageren, J. Schnack, N. S. Dalal, M. Dressel, *Coord. Chem. Rev.* **2009**, *253*, 2315; b) S. Cardona-Serra, J. M. Clemente-Juan, E. Coronado, A. Gaita-Ariño, A. Camón, M. Evangelisti, F. Luis, M. J. Martínez-Pérez, J. Sesé, *J. Am. Chem. Soc.* **2012**, *134*, 14982.

[6] a) Q. G. Zhai, X. Y. Wu, S. M. Chen, Z. G. Zhao, C. Z. Lu, *Inorg. Chem.* **2007**, *46*, 5046; b) Z. Han, Y. Gao, C. Hu, *Cryst. Growth Des.* **2008**, *8*, 1261; c) R. Yu, X. FeiKuang, X. Y. Wu, C. Z. Lu, J. P. Donahue, *Coord. Chem. Rev.* **2009**, *253*, 2872; d) M. Wei, X. Wang, X. Duan, *Chem. Eur. J.* **2013**, *19*, 1607; e) G. C. Liu, Y. F. Wang, A. X. Tian, X. L. Wang, J. J. Cao, S. Yang, H. Y. Lin, *Z. Anorg. Allg. Chem.* **2013**, *639*, 148; f) M. Mirzaei, H. Eshtiagh-Hosseini, N. Lotfian, A. R. Salimi, A. Bauzá, R. Van Deun, R. Decadt, M. Barceló-Oliverb, A. Frontera, *Dalton Trans.* **2014**, *43*, 1906.

[7] a) X. Wang, Y. Guo, Y. Li, E. Wang, C. Hu, N. Hu, *Inorg. Chem.* **2003**, *42*, 4135; b) C. Liu, F. Luo, N. Liu, Y. Cui, X. Wang, E. Wang, J. Chen, *Cryst. Growth Des.* **2006**, *6*, 2658; c) M. Wei, C. He, Q. Sun, Q. Meng, C. Duan, *Inorg. Chem.* **2007**, *46*, 5957; d) C. M. Granadeiro, R. A. S. Ferreira, P. C. R. Soares-Santos, L. D. Carlos, H. S. Nogueira, *Eur. J. Inorg. Chem.* **2009**, 5088; e) H. An, Z. Han, T. Xu, *Inorg. Chem.* **2010**, *49*, 11403; f) H. An, H. Zhang, Z. Chen, Y. Li, X. Liu, H. Chen, *Dalton Trans.* **2012**, *41*, 8390; g) W. F. Zhao, C. Zou, L. X. Shi, J. C. Yu, G. D. Qian, C. D. Wu, *Dalton Trans.* **2012**, *41*, 10091.

[8] a) C. D. Wu, C. Z. Lu, H. H. Zhuang, J. S. Huang, *J. Am. Chem. Soc.* **2002**, *124*, 3836; b) J. Y. Niu, M. L. Wei, J. P. Wang, D. B. Dang, *Eur. J. Inorg. Chem.* **2004**, 160; c) H. Y. An, Y. G. Li, D. R. Xiao, E. Wang, C.-Y. Sun, *Cryst. Growth Des.* **2006**, *6*, 1107.

[9] a) A. Dolbecq, C. Mellot-Draznieks, P. Mialane, J. Marrot, G. Férey, F. Sécheresse, *Eur. J. Inorg. Chem.* **2005**, 3009; b) X. L. Hao, M. F. Luo, W. Yao, Y. G. Li, Y. H. Wang, E. Wang, *Dalton Trans.* **2011**, *40*, 5971; c) K. Wang, D. Zhang, J. Ma, P. Ma, J. Y. Niu, J. P. Wang, *CrystEngComm* **2012**, *14*, 3205; d) S. Zhang, K. Wang, D. Zhang, P. Ma, J. Y. Niu, J. P. Wang, *CrystEngComm* **2012**, *14*, 8677.

 © 2014 Wiley-VCH Verlag GmbH & Co. KGaA, Weinheim

[10] a) L. Jian, E. Shen, Y. Li, D. Xiao, E. Wang, L. Xu, *Cryst. Growth Des.* **2005**, *5*, 65; b) C. Qin, X. Z. Song, S. Q. Su, S. Dang, J. Feng, S. Y. Song, Z. M. Hao, H. J. Zhang, *Dalton Trans.* **2012**, *41*, 2399; c) Y. Xu, Y. Gao, W. Wei, Z. Wang, S. Lia, C. Hu, *Dalton Trans.* **2013**, *42*, 5228.
[11] a) C. H. Li, K. L. Huang, C. W. Hu, Y. N. Chi, X. Liu, Z. G. Han, L. Shen, *Inorg. Chem.* **2009**, *48*, 2010; b) Y. Gao, Y. Xu, Z. Han, C. Li, Y. Chi, C. Hu, F. Cui, *J. Solid State Chem.* **2010**, *183*, 1000; c) X. Liu, Y. Jia, Y. Zhang, R. Huang, *Eur. J. Inorg. Chem.* **2010**, 4027; d) S. Li, D. Zhang, Y. Guo, P. Ma, J. Zhao, J. Wang, J. Niu, *Eur. J. Inorg. Chem.* **2011**, 5397; e) X. Chen, Y. Chen, Z. Xia, H. Hu, Y. Sun, W. Huang, *Dalton Trans.* **2012**, *41*, 10035; f) X. Liu, L. Wang, X. Yin, R. Huang, *Eur. J. Inorg. Chem.* **2013**, 2181.
[12] P. M. Forster, A. R. Burbank, C. Livage, G. Féreyb, A. K. Cheetham, *Chem. Commun.* **2004**, 368.
[13] R. Thouvenot, M. Fournier, R. Franck, G. Rocchiccioli-Deltcheff, *Inorg. Chem.* **1984**, *23*, 598.
[14] a) K. Y. Matsuoto, A. Kobayashi, Y. Sasaki, *Bull. Chem. Soc. Jpn.* **1975**, *48*, 3146; b) M. Sadakane, M. H. Dickman, M. T. Pope, *Angew. Chem.* **2000**, *39*, 3036.
[15] E. Shen, J. Lu, Y. Li, E. Wang, C. Hu, L. Xu, *J. Solid State Chem.* **2004**, *177*, 4372.
[16] A. Frontera, *Coord. Chem. Rev.* **2013**, *257*, 1716.
[17] a) G. A. Bain, J. F. Berry, *J. Chem. Educ.* **2008**, *85*, 532; b) O. Kahn, *Molecular Magnetism*, VCH Publishers, New York, **1993**.
[18] a) D. Gatteschi, C. Benelli, *Chem. Rev.* **2002**, *102*, 2369; b) Y. Wang, X.-L. Li, T.-W. Wang, Y. Song, X.-Z. You, *Inorg. Chem.* **2010**, *49*, 969; c) M. Andruh, E. Bakalbassis, O. Kahn, J. C. Trombe, P. Porcher, *Inorg. Chem.* **1993**, *32*, 1616; d) J. Chakraborty, A. Ray, G. Pilet, G. Chastanet, D. Luneau, R. F. Ziessel, L. J. Charbonnière, L. Carrella, E. Rentschler, M. S. El Fallah, S. Mitra, *Dalton Trans.* **2009**, 10263; e) J. Lhoste, A. Pérez-Campos, N. Henry, T. Loiseau, P. Rabu, F. Abraham, *Dalton Trans.* **2011**, *40*, 9136; f) W. Feng, Y. Zhang, Z. Zhang, X. Lü, H. Liu, G. Shi, D. Zou, J. Song, D. Fan, W.-K. Wong, R. A. Jones, *Inorg. Chem.* **2012**, *51*, 11377; g) M. Hołyńska, M. Korabik, *Eur. J. Inorg. Chem.* **2013**, 5469; h) P. Przychodzeń, K. Lewiński, R. Pełka, M. Bałanda, K. Tomala, B. Sieklucka, *Dalton Trans.* **2006**, 625; i) P. Hu, X. Wang, Y. Ma, Q. Wang, L. Li, D. Liao, *Dalton Trans.* **2014**, *43*, 2234; j) X.-D. Yang, C.-H. Zhang, D.-P. Wang, Y.-G. Chen, *Inorg. Chem. Commun.* **2010**, *13*, 1350.
[19] *X-AREA:* Program for the Acquisition and Analysis of Data, version 1.30, Stoe & Cie GmbH, Darmstadt, Germany, **2005**.
[20] L. J. Farrugia, *J. Appl. Crystallogr.* **2012**, *45*, 849.
[21] G. M. Sheldrick, *SHELX97: Program for Crystal Structure Solution and Refinement*, University of Göttingen, Germany, **1997**.
[22] A. L. Spek, *Acta Crystallogr., Sect. D* **2009**, *65*, 148.

Received: July 26, 2014
Published Online: October 28, 2014

 © 2014 Wiley-VCH Verlag GmbH & Co. KGaA, Weinheim